INSTITUTE OF PHYSICS PUBLISHING JOURNAL OF PHYSICS: CONDENSED MATTER

J. Phys.: Condens. Matter **16** (2004) 5803–5814 PII: S0953-8984(04)76025-7

Low temperature phase transitions and crystal structure of $Na_{0.5}CoO_2$

Q Huang[1], M L Foo[2], J W Lynn[1], H W Zandbergen[3], G Lawes[4], Yayu Wang[5], B H Toby[1], A P Ramirez[6], N P Ong[5] and R J Cava[2]

[1] Center for Neutron Research, NIST, Gaithersburg, MD 20899, USA
[2] Department of Chemistry, Princeton University, Princeton, NJ 08544, USA
[3] National Centre for HREM, Department of Nanoscience, Delft University of Technology, 2628 AL Delft, The Netherlands
[4] Department of Thermal Physics, Los Alamos National Laboratory, Los Alamos, NM 87544, USA
[5] Department of Physics, Princeton University, Princeton, NJ 08544, USA
[6] Lucent Technologies Bell Laboratories, Murray Hill, NJ 07574, USA

Received 6 February 2004
Published 30 July 2004
Online at stacks.iop.org/JPhysCM/16/5803
doi:10.1088/0953-8984/16/32/016

Abstract

Specific heat measurements on $Na_{0.5}CoO_2$ show that the transitions observed at 87 and 53 K in the resistivity and magnetic susceptibility are accompanied by changes in entropy, whereas the one near 20 K is not. Electron diffraction studies suggest that the 87 K transition has a structural component. The crystal structure of $Na_{0.5}CoO_2$, determined by powder neutron diffraction, consists of layers of edge-shared CoO_6 octahedra in a triangular lattice, with Na ions occupying ordered positions in the interleaving planes. The Na ions form one-dimensional zigzag chains. Two types of Co ions are also found in chains.

1. Introduction

Investigations of the copper oxide superconductors have revealed much about the unexpected behaviour of charge transport in square lattices. Though triangle-based lattices have been studied in electrically insulating geometrically frustrated magnets for some time [1–3], conductive layered triangular lattices have not emerged for detailed study until recently, with the discovery of a surprisingly high thermopower in the hexagonal symmetry metallic conductor $Na_{0.7}CoO_2$ [4]. This compound consists of triangular layers of cobalt between close-packed layers of oxygen, resulting in an array of edge-shared CoO_6 octahedra, separated by layers of Na that partially fill sites in the hexagonal plane between the layers of CoO_6 octahedra. The large thermopower has been shown to be due to the transport of spin entropy [5]. Interest was further stimulated in this compound by the discovery of superconductivity at 4.5 K in

$Na_{0.3}CoO_2{\cdot}1.3H_2O$ [6] at a different level of electronic band filling than gives rise to the high thermopower in the same cobalt oxide plane in $Na_{0.7}CoO_2$.

In order to study the transition between the high thermopower state and the host state for the superconductivity, we recently completed a transport-based study [7] of the electronic phase diagram for single crystals of non-hydrated Na_xCoO_2 for $0.3 < x < 0.75$. The data revealed a crossover in properties from an unusual Curie–Weiss metal near $x = 0.7$ to a paramagnetic metallic state for $x = 0.3$. A distinct compound at $Na_{0.5}CoO_2$, which has a transition to an insulating state at 53 K, separates the two metallic regimes at higher and lower sodium concentrations. Characterization of $Na_{0.5}CoO_2$ by electron diffraction revealed the presence of an orthorhombic symmetry supercell, which was attributed to Na ordering and an associated charge ordering of the underlying Co. The structures of Na_xCoO_2 prepared under different conditions and at different stoichiometries have been described [8–11], but the ordered phase at $x = 0.5$ has not been previously characterized. Here we report specific heat measurements on $Na_{0.5}CoO_2$ to characterize further the low temperature phase transitions, and electron diffraction patterns showing the presence of a structural distortion at low temperature. In addition, the average crystal structure of $Na_{0.5}CoO_2$, determined at 300 and 3.5 K by neutron powder diffraction, is reported. Two types of Co chains, associated with zigzag chains of Na running along one crystallographic direction, are found.

2. Experimental details

Compounds with the γ-Na_xCoO_2 structure type, the host phase for the superconductor and the thermoelectric, can be synthesized only in the range of stoichiometry $0.7 < x < 0.8$ by conventional thermodynamic methods. Lower x contents of the same structure type are synthesized by chemical deintercalation of Na at room temperature. The $Na_{0.5}CoO_2$ powder employed here for the neutron diffraction, specific heat and susceptibility measurements was synthesized from single-phase powder of $Na_{0.75}CoO_2$ prepared by heating appropriate proportions of Na_2CO_3 and Co_3O_4 overnight in flowing oxygen at 800 °C. That powder was then treated by immersion (with stirring) in acetonitrile saturated with I_2 in sufficient excess to insure full oxidation of the powder to $Na_{0.5}CoO_2$. The powder was then washed with acetonitrile and stored in a dry environment for all subsequent handling. Small single crystals of $Na_{0.5}CoO_2$ were obtained by the same method by starting with floating-zone grown crystals of $Na_{0.75}CoO_2$. Further details have been described elsewhere [7].

Magnetization measurements were carried out between 300 and 1.8 K in an applied field of 1 kOe, employing a Quantum Design MPMS magnetometer. Standard four-contact resistivity measurements were carried out on small single crystals (approximately 1 mm × 2 mm × 0.1 mm) between 300 and 2 K. Specific heat was measured between 2 and 150 K on a polycrystalline powder of total mass 0.1 g, mixed with silver powder to insure thermal contact, in a Quantum Design PPMS system. The specific heat of the silver powder and the addenda were measured separately and subtracted from the raw data for $Na_{0.5}CoO_2$. Electron diffraction measurements were performed in Philips CM300UT and CM200ST electron microscopes, both equipped with a field emission gun. Nanodiffraction was performed using a condenser aperture of 10 μm and an electron probe size of 10–30 nm in diameter. The specimen cooling experiments were performed using a custom-made holder for operation at about 100 K.

The neutron powder diffraction intensity data for $Na_{0.5}CoO_2$ were collected using the BT-1 high-resolution powder diffractometer at the NIST Center for Neutron Research, employing a Cu(311) monochromator to produce a neutron beam of wavelength 1.5403(1) Å. Collimators with horizontal divergences of 15′, 20′ and 7′ of arc were used before and after

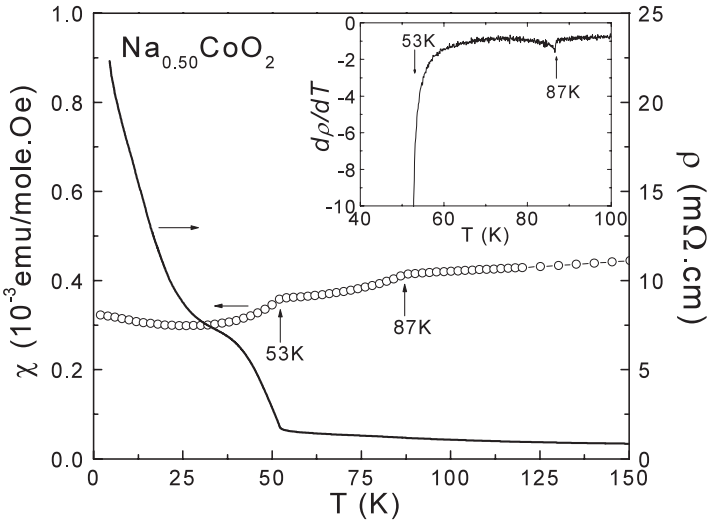

Figure 1. The magnetic and resistive characterization of the phase transitions in $Na_{0.5}CoO_2$ below 100 K. The resistive data are taken on a single crystal, measured in the CoO_2 plane. The magnetic susceptibility data are taken on the polycrystalline sample employed in the specific heat and neutron diffraction studies.

the monochromator, and after the sample, respectively. The intensities were measured in steps of 0.05° in the 2θ range 3°–168°. Data were collected at a variety of temperatures from 300 to 3.5 K to elucidate the possible magnetic and crystal structure transitions. The structural parameters were refined using the program GSAS [12]. The neutron scattering amplitudes used in the refinements were 0.363, 0.253 and 0.581 ($\times 10^{-12}$ cm) for Na, Co and O, respectively.

3. Results

Figure 1 shows the resistive and magnetic characterization of the low temperature phase transitions in $Na_{0.5}CoO_2$. The resistivity measured in the CoO_2 plane increases significantly on cooling at an onset temperature of approximately 53 K. After a slight saturation, the slope of the ρ versus T curve increases with cooling below 25 K, indicating another phase transition. The magnetic susceptibility, on the other hand, shows decreases at 87 and 53 K, but no features near 20 K. The 87 K phase transition can be observed in the resistivity data, but only by taking the derivative of the curve (inset, figure 1). Characterization of $Na_{0.5}CoO_2$ by μSR has indicated the onset of magnetic ordering at 53 K, resolving further into the ordering of two distinct types of magnetic atoms at 20 K. No magnetic ordering was associated with the 87 K transition [13].

Specific heat characterization of the phase transitions is shown in figures 2 and 3. For the 87 K transition, a distinct peak is observed, characteristic of a three-dimensional phase transition. For the transition at 53 K, the specific heat change is more subtle, and appears to be somewhat broader in temperature than the 87 K transition. Figure 3 shows in the main panel that there is no specific heat anomaly for the 20 K transition, indicating no substantial change in magnetic entropy and suggesting that this may be a spin reorientation transition. The integrated entropy in the very small peak at 3 K is approximately that expected for 0.1% or less of the ordering of spin 1/2 particles. Low temperature susceptibility measurements (inset) show no transition at that temperature, suggesting that the 3 K feature is very likely due to the presence of a very small amount of impurity phase.

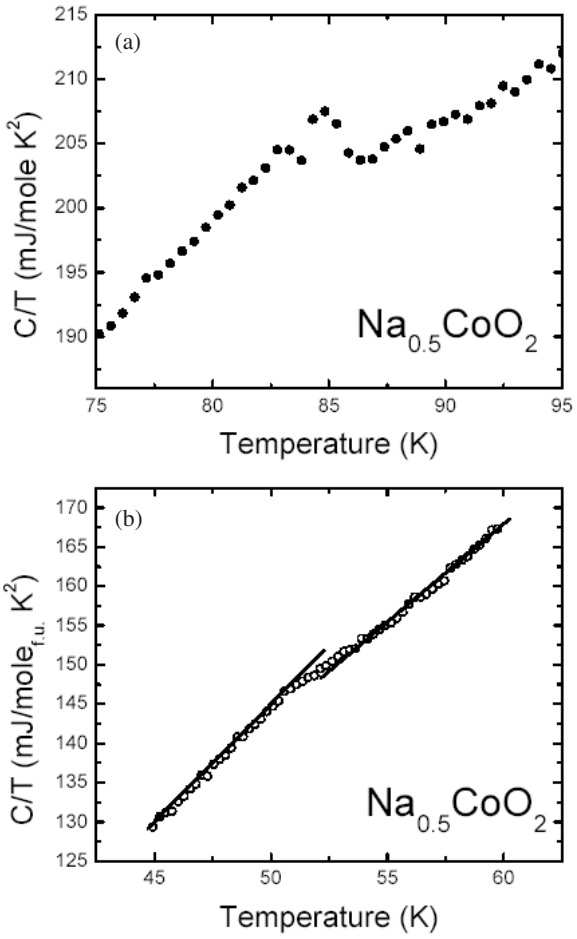

Figure 2. Thermodynamic characterization of the 87 and 53 K transitions in $Na_{0.5}CoO_2$.

Figure 4 shows electron diffraction patterns for $Na_{0.5}CoO_2$. Panels 4(a)–(c) show the diffraction patterns in the $hk0$, $h0l$ and $0kl$ reciprocal lattice planes at room temperature. These patterns, and electron diffraction tilt series, show the presence of the basic hexagonal symmetry subcell, arising from the two-layer CoO_2 triangular network and the average Na distribution in the γ-Na_xCoO_2 structure type, and, in addition, an orthorhombic supercell. Electron diffraction patterns show as systematic extinctions: for $hk0$, $k = 2n$ (not visible in the [001] diffraction pattern due to multiple scattering, but a tilt exciting only the $0k0$ lines shows this extinction), for $h0l$ none and for $0kl$ k and l both even. The latter extinction condition is more exclusive (a combination of an n glide plane and a b glide plane) than those of a normal three-dimensional space group. Electron diffraction studies have shown [14] that the commensurate superlattice at $x = 0.5$ evolves continuously to an incommensurate superlattice with small changes in Na content induced during electron beam irradiation. This indicates that a continuously varying structural modulation that is a function of Na content, best represented by a four-dimensional space group, has locked into a commensurate modulation at $x = 0.5$. Panels 4(a) and (d) show the room temperature and low temperature [001] ($hk0$) electron diffraction patterns for $Na_{0.5}CoO_2$. The cooling stage is expected to reach temperatures on

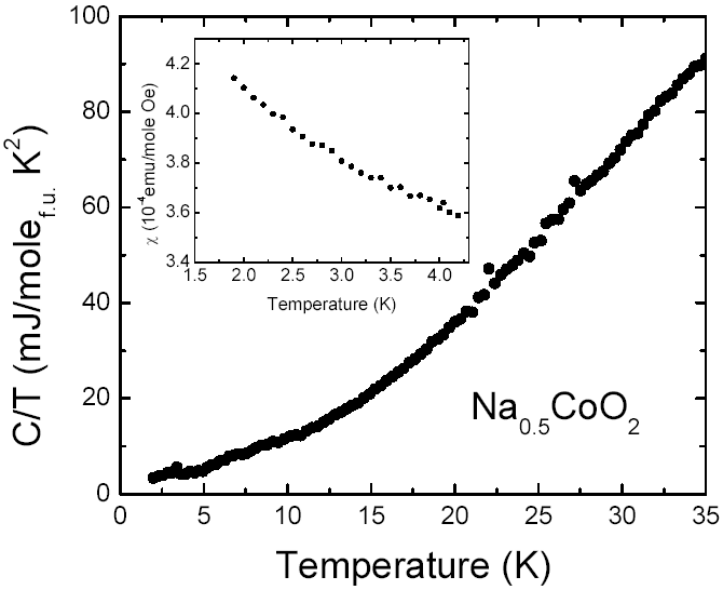

Figure 3. Specific heat in the vicinity of the 20 K transition. Inset, the magnetic susceptibility at low temperatures.

the order of 100 ± 20 K. The ambient temperature electron diffraction pattern (figure 4(a)) shows the orthorhombic $a\sqrt{3}, 2a$ supercell. Extra diffraction spots are clearly seen in the low temperature diffraction pattern (figure 4(d)), indicative of a structural distortion at low temperatures in which both the a and b axes of the orthorhombic cell are tripled. These spots are not observed in all crystallites in the sample. This suggests that such super-supercell ordering may be susceptible to damage by the electron beam, or exist over only a narrow range of temperature, or that compositional inhomogeneities make it favourable in some areas but not in others. The intensity of the extra spots is substantially weaker than those of the hexagonal substructure spots and the orthorhombic superstructure spots, indicating the subtlety of the structural distortion. This distortion may be associated with the 87 K phase transition observed in other characterization experiments, but we have not unambiguously determined whether that is the case. In conjunction with the other data, these data suggest that this transition may be associated with the formation of a charge density wave or orbital ordering. Further study will be required to characterize this super-supercell ordering in more detail.

A structural model for $Na_{0.5}CoO_2$ in the basic γ-Na_xCoO_2 structure type, with hexagonal $P6_3/mmc$ symmetry and lattice parameters $a \approx 2.81$ and $c \approx 11.1$ Å, was used as the starting point in the structural refinement employing the neutron diffraction data. The model gives a good fit to all the strongest intensity peaks, with the Na atoms distributed in a disordered fashion in the $2b$ and $2c$ sites within the $P6_3/mmc$ symmetry space group with the occupancy parameter of approximately 0.25 for both sites. The neutron diffraction data show a substantial number of additional weak Bragg peaks (about 1% of the strongest peak). These peaks can be indexed by the orthorhombic supercell seen in the ambient temperature electron diffraction patterns, with $a_o = \sqrt{3}a_H$, $b_o = 2a_H$ and $c_o = c_H$, where a_H and c_H are hexagonal subcell parameters. Figure 5 shows a portion of the neutron powder diffraction pattern for $Na_{0.5}CoO_2$ at 295 K on an expanded vertical scale. Bragg peak positions are shown by the vertical lines for $Na_{0.5}CoO_2$ (top) and for a CoO impurity (bottom). Peaks with shorter vertical lines are the

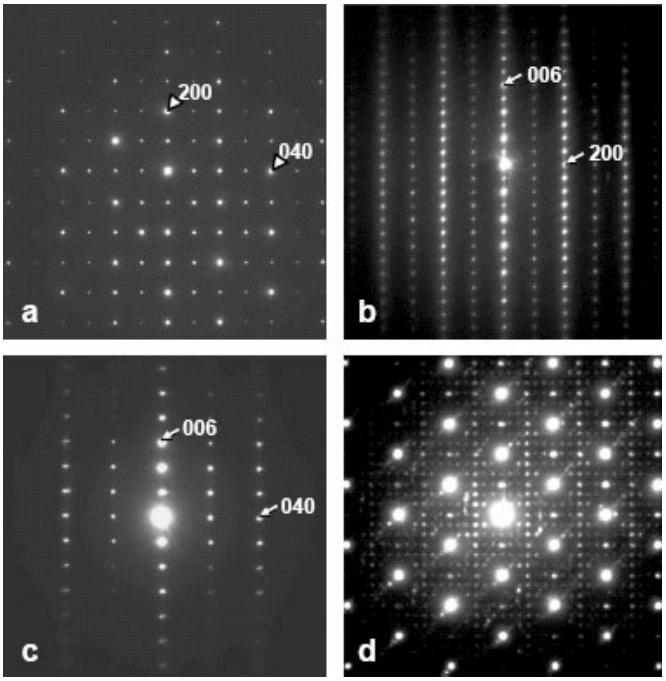

Figure 4. Electron diffraction patterns of $Na_{0.5}CoO_2$. (a)–(c) The room temperature diffraction patterns of the orthorhombic $a\sqrt{3}$, $2a$ superstructure. (a) $hk0$ plane, (b) $h0l$ plane and (c) $0kl$ plane. (d) Diffraction pattern in the $hk0$ plane taken at about 80–100 K. The extra reflections require a tripling of both the a and b axes of the ambient temperature orthorhombic unit cell. Note that in panels (a) and (b), the $0k0$ reflections with k odd and the $00l$ reflections with l odd are seen due to multiple scattering: if the crystal is tilted such that only the $0k0$ line or the $00l$ line is excited, then the k odd or l odd reflections disappear.

superlattice peaks. The indices of the observed reflections are consistent with those observed in the electron diffraction patterns. The two possible primitive orthorhombic space groups with those reflection conditions are $Pn2_1m$ (#31) and $Pnmm$ (#59). Comparable quality fits of the final structural model to the observed data were obtained using both space groups. For the final results, the $Pnmm$ space group was used due to its higher symmetry and fewer independent variables.

The resulting superstructure model having $Pnmm$ symmetry and the Na atoms completely ordered (figures 6 and 7) was derived initially based on semi-quantitative analysis of the electron diffraction data, and tested quantitatively with the neutron diffraction data. The model provides a very good fit to the neutron diffraction data, and represents the average crystal structure of $Na_{0.5}CoO_2$. The refined structural parameters and selected bond distances and angles are shown in table 1. Figures 5 and 8 show a good fit of the calculated intensities to the observed neutron powder diffraction pattern at 295 K. We note that our instrumental resolution is insufficient to resolve any metric deviations from the ideal $a_o = \sqrt{3}a_H$, and $b_o = 2a_H$ relationships, and therefore the orthorhombic a and b axes were not varied independently in the structural refinements. Also, due to the hexagonal pseudosymmetry, some of the positional parameters for some atoms were constrained to be fixed at ideal positions for the final refinements. There is no indication of substantial deviations from these ideal positions. Though the average structure is well described in the present analysis, elucidation of finer details will have to await higher resolution structural studies.

Table 1. Structural parameters and selected bond distances (Å) and angles (degrees) for $Na_{0.5}CoO_2$ at 295 K (first line) and 3.5 K (second line). Space group: $Pnmm$ (#59)[a,b] [$Pnmm\langle$**bca**$\rangle Pmmn$ (origin choice 2)].

$a = 4.876\,18(5)$	$b = 5.630\,53(9)$	$c = 11.1298(2)$ Å			
$4.875\,70(4)$	$5.629\,97(7)$	$11.0634(2)$			
Atom	Site	x	y	z	B (Å^2)
Co(1)	4f	0	1/4	0	0.49(3)
		0	1/4	0	0.23(2)
Co(2)	4d	1/2	0	0	0.49(3)
		1/2	0	0	0.23(2)
Na(1)	2b	−0.027(2)	1/4	3/4	1.7(1)
		−0.018(2)	1/4	3/4	0.79(6)
Na(2)	2a	0.361(2)	3/4	3/4	1.7(1)
		0.352(2)	3/4	3/4	0.79(6)
O(1)	4f	1/3*	1/4	0.0894(1)	0.51(1)
		1/3*	1/4	0.0895(1)	0.29(1)
O(2)	4f	1/3*	3/4	0.0816(3)	0.51(1)
		1/3*	3/4	0.0820(3)	0.29(5)
O(3)	8g	−1/6*	0*	0.0894(1)	0.51(1)
		−1/6*	0*	0.0895(1)	0.29(1)
Selected bond distances and angles (295 K only)					
Co(1)–O(1)		1.9059(6)	O(1)–Co(1)–O(3)	95.22(4)	
Co(1)–O(2)		1.862(6)	O(2)–Co(1)–O(3)	96.76(5)	
Co(1)–O(3)	×4	1.9059(6)	O(3)–Co(1)–O(3)	95.22(4)	
Co(2)–O(1)	×2	1.9059(3)	O(1)–Co(2)–O(2)	96.76(5)	
Co(2)–O(2)	×2	1.862(3)	O(1)–Co(2)–O(3)	95.22(4)	
Co(2)–O(3)	×2	1.9059(6)	O(2)–Co(2)–O(3)	96.76(4)	
Na(1)–O(2)	×2	2.396(7)			
Na(1)–O(3)	×4	2.464(4)			
Na(2)–O(1)	×3	2.328(7)			
Na(2)–O(3)	×3	2.464(4)			
• $R_p = 3.13\%$	$R_{wp} = 3.85\%$	$\chi^2 = 1.250$			
3.35	4.11	1.288			

[a] Due to high correlations: (1) Structural parameters were constrained to be $a/b = \sqrt{3}/2$, and $z(O(1)) = z(O(3))$. (2) Temperature factors for Co, Na and O were constrained to be equal, respectively. (3) * Parameters fixed to hexagonal pseudosymmetry positions.

[b] In the standard setting (295 K data): Space group $Pmmn$, $a = 5.6305$, $b = 11.1299$, $c = 4.8758$.

Atom	x	y	z
Co(1)	1/4	0	0
Co(2)	0	0	1/2
Na(1)	1/4	3/4	−0.027
Na(2)	3/4	3/4	0.361
O(1)	1/4	0.0894	1/3
O(2)	3/4	0.0816	1/3
O(3)	0	0.0894	−1/6

The crystal structure of $Na_{0.5}CoO_2$ is unexpected. In the simplest case, if Na positions are determined by ion–ion repulsion within the Na layer, then a triangular Na lattice is expected for $x = 1/3$, but $x = 1/2$ is not expected to yield a special case of long range ordering. In

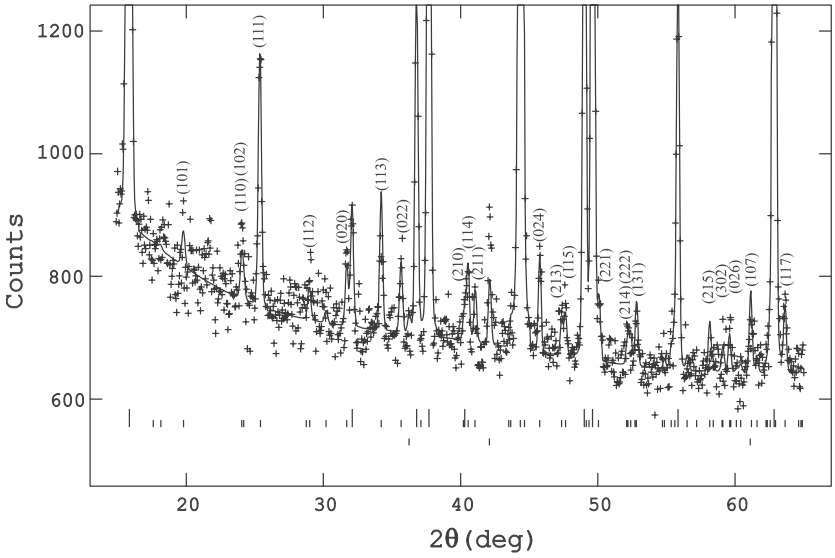

Figure 5. Portion of the observed (crosses) and calculated (solid curve) powder neutron diffraction intensities for $Na_{0.5}CoO_2$ on an expanded vertical scale at 295 K. The fit is for the superstructure model with *Pnmm* symmetry. The possible Bragg peak positions are shown by the vertical lines for $Na_{0.5}CoO_2$ (top) and for CoO impurity (bottom). Peaks with index and shorter vertical lines are the superlattice peaks.

Na_xCoO_2, however, the availability of two types of Na sites that have comparable energies adds an extra degree of freedom to the possible structures. Both Na positions are trigonal prismatic sites, but one trigonal prism shares edges with adjacent CoO_6 octahedra (Na2), while the other trigonal prism shares faces with adjacent CoO_6 octahedra (Na1). The Na2 site is preferred for a broad range of Na contents in Na_xCoO_2 [8–11], but for $Na_{0.5}CoO_2$ we find the Na1 and Na2 sites are occupied in equal ratios.

Figures 9(a) and (b) show the structure from different perspectives. The first is based on a central Co plane, and the Na layers above and below it, and shows the zigzag chains of Na and the parallel chains of Co over several unit cells. The second extracts the Na atoms in the ordered layer only. This figure shows that the Na lattice is in fact a distorted hexagonal lattice. To make the lattice into an ideal hexagonal arrangement, which would minimize the Na^+–Na^+ Coulomb repulsions, the Na ions would be forced into unfavourably shaped Na–O coordination polyhedra. Thus the geometry the Na displays must involve in part a compromise between ion–ion repulsion and optimally shaped Na–O coordination polyhedra.

This kind of compromise cannot explain, however, why an ordered structure would form at all at this composition. We conclude that Na_xCoO_2 at $x = 0.5$ is a special composition for electronic reasons, as is borne out by its unique magnetic and electronic properties. The crystal structure determination reinforces this interpretation because two distinct types of Co atoms are seen, with the parallel chain configuration already described. We postulate that the Na 'decorates' the particular Co chains in which the formal Co oxidation state is lower. Thus the final Na configuration is a three-way compromise: accommodating the effects of interaction with the underlying Co lattice (whose charge configuration we believe to be determined by a fundamental electronic instability), the mutual repulsion of the Na ions in the layer, and the locations of Na–O coordination polyhedra of favourable shape.

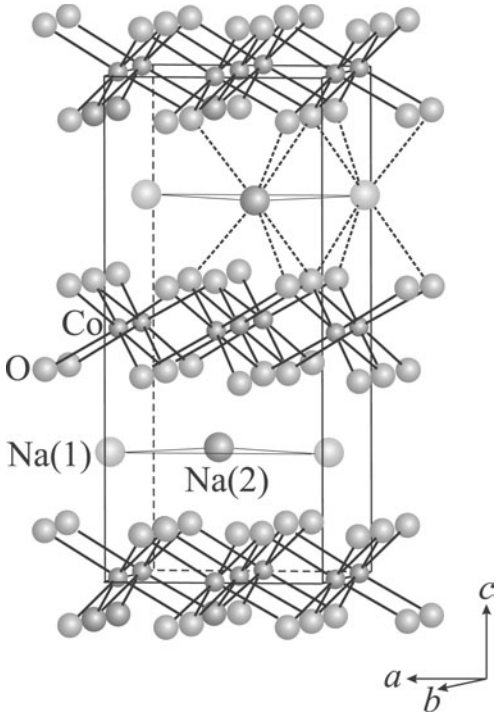

Figure 6. The crystal structure of $Na_{0.5}CoO_2$, showing layers of edge-shared CoO_6 octahedra and the triangular prismatic coordination of Na within the intermediary layers.

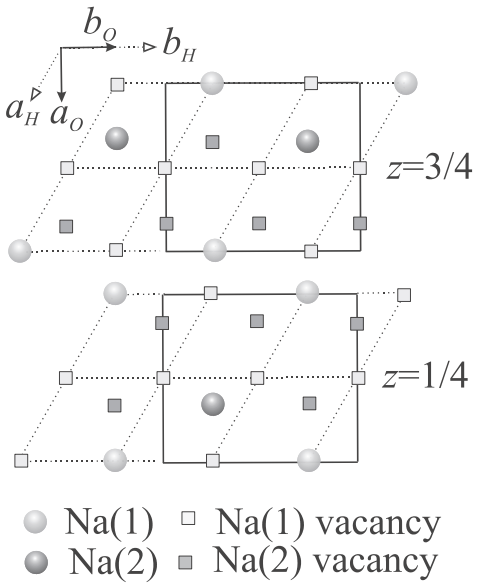

Figure 7. The Na ion configuration for $Na_{0.5}CoO_2$. The dotted lines show the *ab* plane of the hexagonal subcell, and the solid lines indicate the orthorhombic supercell.

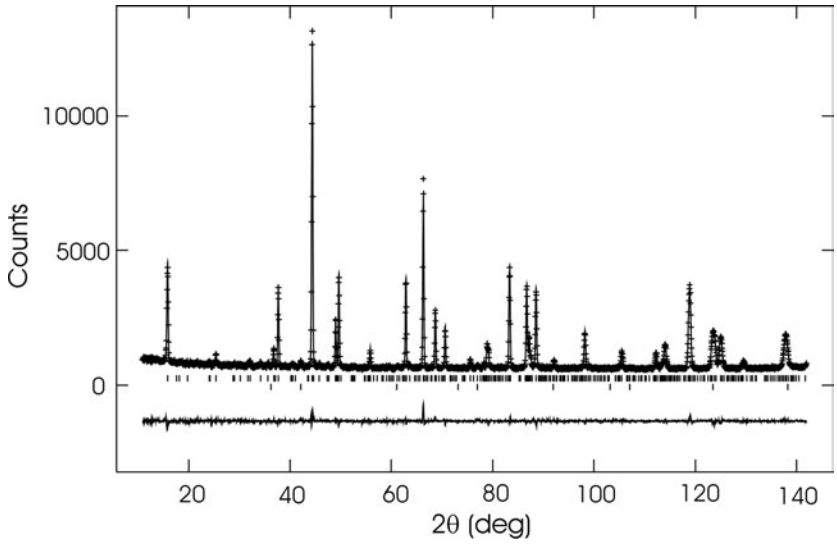

Figure 8. Observed (crosses) and calculated (solid curve) intensities for $Na_{0.5}CoO_2$ at 295 K. Differences between the observed and calculated intensities are shown at the bottom of the figure. The vertical curves indicate the Bragg peak positions for $Na_{0.5}CoO_2$ (upper) and 1 wt% CoO (lower).

The present refinement of the structure of $Na_{0.5}CoO_2$ is not sufficiently precise to determine the details of the shapes of the Co–O coordination polyhedra, expected to be a sensitive measure of the electronic state of the system. At the level of precision afforded by the present data, two different types of Co atoms are found in chains in $Na_{0.5}CoO_2$. Co1 has one shorter and five longer bonds to oxygen, whereas Co2 has two shorter and four longer bonds to oxygen. This indicates that the Co1 is lower in formal oxidation state than Co2—i.e. that there is charge ordering in the CoO_2 plane. The Na in the planes below and above the Co plane, while bonded to O in the coordination polyhedra of both Co1 and Co2, are coordinated to a larger fraction of the O in the $(Co1)O_6$ polyhedron. This supports our conjecture that the Na chooses to decorate the chain in which the less highly charged Co is present, consistent with Pauling's rules. The differences in observed bond lengths in our refinements are subtle, and it remains to be determined in future work how charge or orbital ordering may be fully manifested in the crystal structure.

4. Conclusion

The Na_xCoO_2 phase diagram naturally divides into two metallic and magnetic regimes, one at high Na content that exhibits unusual spin transport properties, and the other at low Na content that is the host composition for the superconductor. The composition that divides these regimes, $Na_{0.5}CoO_2$, undergoes several phase transitions below 100 K, and becomes a magnetically ordered insulator at low temperatures. The crystal structure involves an ordering of the Na ions into zigzag chains that we postulate decorate charge-ordered chains of Co ions, giving a basis for the highly unusual properties observed. Further diffraction studies would be of great interest to determine the crystal structure in more detail, and to characterize the structural changes that occur at the three phase transitions.

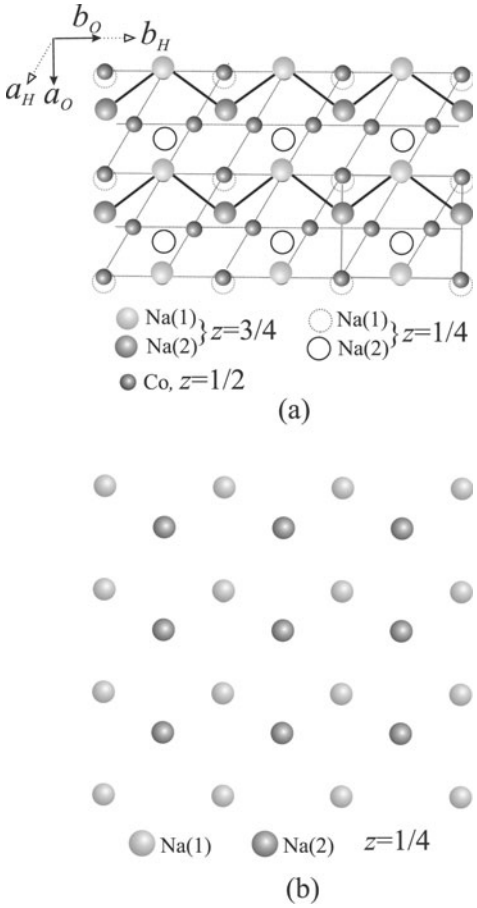

Figure 9. (a) A central layer of Co at $z = 1/2$ with a layer of Na above it (at $z = 3/4$) and below it (at $z = 1/4$) (see also figure 6). The zig–zag Na chain is emphasized as is the hexagonal Co lattice. Oxygen planes are omitted for clarity. (b) The Na ion configuration in a single layer, over several unit cells, in $Na_{0.5}CoO_2$. The distorted hexagonal array is visible.

Acknowledgments

The research at Princeton University was supported by the NSF MRSEC program, grant DMR-0213706, and the NSF Solid State Chemistry Program, grant DMR 0244254. Identification of commercial equipment in the text is not intended to imply recommendation or endorsement by the National Institute of Standards and Technology.

References

[1] Ramirez A P 2001 *Handbook of Magnetic Materials* ed K J H Buschow (New York: New Holland)
[2] Greedan J E 2001 *J. Mater. Chem.* **11** 37
[3] Moessner R 2001 *Can. J. Phys.* **79** 1283
[4] Terasaki I, Sasago Y and Uchinokura K 1997 *Phys. Rev.* B **56** R12685
[5] Wang Y, Rogado N S, Cava R J and Ong N P 2003 *Nature* **423** 425
[6] Takada K, Sakurai H, Takayama-Muromachi E, Izumi F, Dilanian R A and Sasaki T 2003 *Nature* **422** 53
[7] Foo M L, Wang Y, Watauchi S, Zandbergen H W, He T, Cava R J and Ong N P 2003 *Phys. Rev. Lett.* **92** 247001

[8] Delmas C, Braconnier J J, Fouassier C and Hagenmuller P 1981 *Solid State Ion.* **3/4** 165
[9] Fouassier C, Matejka G, Reau J-M and Hagenmuller P 1973 *J. Solid State Chem.* **6** 532
[10] Lynn J W, Huang Q, Brown C M, Miller V L, Foo M L, Schaak R E, Jones C Y, Mackey E A and Cava R J 2003 *Phys. Rev.* B **68** 214516
[11] Jorgensen J D, Avdeev M, Hinks D G, Burley J C and Short S 2003 *Phys. Rev.* B **68** 214517
[12] Larson A and Von Dreele R B 1990 *Internal Report LAUR086-748* Los Alamos National Laboratory
[13] Uemura T J, Russo P L, Savici A T, Wiebe C R, MacDougall G J, Luke G M, Mochizuki M, Yanase Y, Ogata M, Foo M L and Cava R J, unpublished
[14] Zandbergen H W, Foo M L, Xu Q, Kumar V and Cava R J 2004 *Phys. Rev.* B **70** 024101